

Development of a novel microplate for high-throughput screening and optimization of DHA producing strains based on CFD technology

He Shaojie¹, Linhui Yang¹, YuanHang Du¹, LingLing Tong¹, Yue Wang¹, and Guo dongsheng¹

¹Affiliation not available

April 19, 2023

Abstract

Microtiter plates are suitable for screening and process development of most microorganisms. They are currently the container of choice for high-throughput and small-scale microbial culture, but require optimization for specific work. This research presents a novel type of microtiter plate was developed using computational fluid dynamics (CFD) technology. The new plate provides high oxygen supply and optimal mixing effects for the fermentation culture of docosahexaenoic acid (DHA) producing strains, surpassing the conventional method of strains screening with shake flasks, which is insufficient. the shape of the microtiter plate was modified, and baffles were introduced to improve mass transfer and oxygen supply effects in the vibrating bioreactor. CFD technology was used to model the new plate's characteristics, establishing the superiority of hexagonal microtiter plates with six baffles. Parameters in the incubation process, such as vibration frequency and liquid load, were optimized, and the final result achieved a K_{La} of $0.61s^{-1}$ and a volume power input of $2364 w/m^3$, which was 4-5 times better than the original 96-well plate. The culture results optimized by the model were also verified. Therefore, this new microtiter plate provides a powerful tool for future high-throughput screening of strains.

Development of a novel microplate for high-throughput screening and optimization of DHA producing strains based on CFD technology

Shao-Jie He¹, Lin-Hui Yang¹, Yuan-Hang Du¹, Ling-Ling Tong¹, Yue Wang¹, Dong-Sheng Guo^{1*}

¹School of Food Science and Pharmaceutical Engineering, Nanjing Normal University, Nanjing, China

***Corresponding Author:** Dong-Sheng Guo, School of Food Science and Pharmaceutical Engineering, Nanjing Normal University, No. 1 Wenyuan Road, Nanjing 210023, China. **Email** :guodongs@njnu.edu.cn

Abstract : Microtiter plates are suitable for screening and process development of most microorganisms. They are currently the container of choice for high-throughput and small-scale microbial culture, but require optimization for specific work. This research presents a novel type of microtiter plate was developed using computational fluid dynamics (CFD) technology. The new plate provides high oxygen supply and optimal mixing effects for the fermentation culture of docosahexaenoic acid (DHA) producing strains, surpassing the conventional method of strains screening with shake flasks, which is insufficient. the shape of the microtiter plate was modified, and baffles were introduced to improve mass transfer and oxygen supply effects in the vibrating bioreactor. CFD technology was used to model the new plate's characteristics, establishing the superiority of hexagonal microtiter plates with six baffles. Parameters in the incubation process, such as vibration frequency and liquid load, were optimized, and the final result achieved a K_{La} of $0.61s^{-1}$ and a volume power input of $2364 w/m^3$, which was 4-5 times better than the original 96-well plate. The culture

results optimized by the model were also verified. Therefore, this new microtiter plate provides a powerful tool for future high-throughput screening of strains.

Keywords : docosahexaenoic acid, computational fluid dynamics, high-throughput screening, microplate

Abbreviations : CFD, computational fluid dynamics; DHA, docosahexaenoic acid; K_{La} , Oxygen transfer coefficient; ϵ , average turbulent dissipation rate; k , turbulent flow kinetic energy; RSM, response surface methodology; MSG, monosodium glutamate; Yeast, yeast extract; Glu, glucose.

INTRODUCTION

Over the decades, microorganisms have been used as “mini-factories” in biomanufacturing to aid in the diversity of metabolic pathways and their accompanying ability to transform a wide range of renewable raw materials into value-added compounds via fermentation [1-3]. In the quest to obtain DHA from fish oil, species like *Schizochytrium* sp. have been widely used in liquid fermentation due to their short growth cycle and high cell density cultivation in bioreactors [4]. To optimize the culture, the screening of strains like *Schizochytrium* sp. has been done from shake flasks to 5L fermenters. However, this process has many issues, including low optimization throughput, high labor intensity, and unsatisfactory optimization results, which are related to the structure of shake flask and the regulation of parameters in the fermentation process [5-6]. Microplates are commonly used to establish high-throughput technologies in cell line and process development due to their high throughput, low labor intensity, and ease of automation [7-9]. However, the existing microtiter plate can only reach a K_{La} of 0.32 s^{-1} , making it challenging to achieve high-quality fermentation and cultivation [10-11]. Therefore, improving the microtiter plate to adapt to the high-throughput screening of DHA-producing strains is not only an academic goal, but also an urgent need for industrial practice.

The liquid volume in microplates is usually very small, and in most systems, it is impossible to control key system parameters such as K_{La} and turbulence flow energy [10,12]. Additionally, the lack of online monitoring during fermentation makes such systems difficult to use and understand [13]. However, with the rapid development of CFD, its application in biological fermentation has received more attention. By using mathematical modeling and numerical solutions through a computer, it is possible to quantitatively characterize the flow field properties in a bioreactor [14-15]. Therefore, CFD technology has been widely used to simulate flow fields in bioreactors to obtain engineering parameters such as mass transfer, mixing, and shearing [16-18]. Many studies have used CFD to redesign various types of bioreactors through structural improvements and hydrodynamic optimization to meet the needs of microbial culture in industrial applications [19-21]. Therefore, utilizing CFD to characterize key performance indicators like the oxygen mass transfer coefficient, specific surface area and volume power input can visualize the entire growth process of microorganisms and regulate the parameters to optimize the conditions for achieving the best culture effect.

The cross-sections of existing microtiter plate are typically square or circular, which cannot provide sufficient oxygen supply, a critical parameter for microbial screening and process development [22-23]. In addition to increasing the vibration diameter and frequency and reducing the volume of loaded liquid, modifying the geometry of the bioreactor is also an effective way to achieve high efficiency of oxygen transfer and mixing [24]. Many studies have shown that changing the shape of the microtiter plate or introducing baffles can significantly increase the maximum oxygen transfer capacity. For example, Delgado et al. found that a bioreactor with baffles, could increase the maximum oxygen transfer capacity by a factor of 5 to 10, even at lower vibration frequencies [25-28]. However, it has been reported that the parameters of the microbial growth process have not been well characterized, and the reproducibility of growth is poor [29]. Moreover, excessive increases in the vibration frequency during fermentation culture to enhance oxygen supply and mixing can lead to liquid splashing, gas transport restrictions and fermentation pollution [30]. Therefore, in many cases, vibratory bioreactors with other geometries or baffles are not widely used.

This research established a high-throughput screening system for producing DHA based on CFD technology. It involved modeling and analyzing the oxygen supply level and mixing effect of microtiter plates with

different geometries, to evaluate key parameters such as oxygen transfer coefficient, turbulence dissipation rate and volume power input. In addition, the splash height and overflow level of the liquid around the rocking orbit during vibration culture were also monitored in real-time to ensure conditions were stable. The operation parameters were then optimized using the response surface method, and a microplate was constructed using 3D printing technology for culture experiments. The superiority of the hexagonal microtiter plate with six baffles was determined. This research was able to achieve high-throughput screening for DHA-producing strains, which has significant implications for scaling up DHA production in the industry.

MATERIALS AND METHODS

2.1 Microorganisms and culture methods

The industrial DHA producing strains *Schizochytrium* sp., *Aurantiochytrium* sp., and *Thraustochytrium* sp. were used in this study and were obtained from the China Center for Type Culture Collection, stored at -80 °C with 20% (v/v) glycerol.

The media and culture conditions were the same as in our previous studies. The seed medium was artificial seawater supplemented with glucose (50 g/L) and yeast extract (0.4 g/L). The fermentation medium was artificial seawater containing 70 g/L glucose, 1 g/L yeast extract, and 30 g/L glutamate [1].

Culture experiments in the laboratory were performed in 96-well plates. The strains were inoculated in conventional microtiter plates and novel bioreactors. The specific dimensions of the novel microplate are shown in **Figure 1**. The conventional 96-well plates are square or circular cross-sectional microtiter plates commonly used in laboratories.

2.2 Rheological measurement and Staining of cells

To ensure the accuracy of the simulation, it is necessary to make precise measurements of the rheological parameters of the liquid phase [31-32]. Therefore, it is necessary to determine the density, viscosity and surface tension of the fermentation broth of *Schizochytrium* sp. The density was measured using the density meter DM40, the viscosity was determined using the viscometer ROTAVISC lo-vi, and the surface tension was analyzed using the tensile meter k11. Because the biomass of microorganisms varies at different stages of growth, rheological measurements of the organism are required at each time point to obtain accurate rheological properties.

The staining of bacterial species was performed using Nile red staining for intracellular lipid. 1 mg Nile red (MACKLIN) was dissolved in 10 mL of acetone and stored away from light. A certain amount of culture solution was mixed with dimethyl sulfoxide, then Nile red solution was added and stained in the dark. The fluorescence intensity was measured using a multifunctional microplate reader.

2.3 CFD simulation

All simulations were performed using ANSYS FLUENT software (ANSYS, USA). ANSYS ICEM software was used to create the mesh and refine the model boundaries to improve the accuracy of computer numerical calculations. The medium was modeled as a Newtonian fluid with density and viscosity based on the actual fermentation broth.

2.3.1 Model Settings

Two phases, liquid and gas, exist inside the microtiter plate and have a clear distinct interface. In this study, the Volume of Fluid (VOF) model was used to track the gas-liquid interface. This classic multiphase flow model simulates non-mixing and distinct interfaces and has been used in many studies to simulate the motion

of vibrating bioreactors, proving to be an effective method for fluid evaluation [33-34]. The rotational motion of the microtiter plate drives the internal liquid to rotate, leading to a gas-liquid interface with high strain rate and high distortion. The RNG k- ϵ turbulent transport model is suitable for describing the turbulent motion.

In order to improve the accuracy of the calculation process, such as the influence of the model mesh number on the solution results, the mesh size was established as 5.5×10^6 computational units. Three interfacial compression levels were tested simultaneously to simulate the air-liquid interface more realistically. The solver was set to run for at least 5 seconds, and the average turbulent energy dissipation rate was monitored to ensure that the simulation could reach quasi-steady state.

2.3.2 Microtiter plate motion model

The movement of the microplate is usually a rotary movement driven by the device. In order to calculate the distribution of liquid in the case of rotary motion, Buchs et al. described the movement of liquid as a superposition of two motion processes: on the one hand, the liquid moves in a circular motion with a certain radius; on the other hand, the liquid rotates around the center of the microplate. These two movements work together to make the liquid move periodically in a fixed direction. Many studies used the dynamic grid method to simulate this movement, but the dynamic grid requires mesh reconstruction at each step of the calculation, resulting in a large amount of resource consumption and low efficiency.

This paper used another way to simulate this motion process. The movement of microtiter plates is mainly subjected to two forces: gravity and centrifugal force. The movement of the microplate generates centrifugal force, which drives the liquid to move, thus forming a gas-liquid interface. Therefore, it can be assumed that the microplate is stationary and the liquid rotates under a combination of periodic centrifugal force and a gravitational force. Periodic centrifugal force can be described in the following two equations [35]:

$$F_x = \omega^2 r \cos(\omega\tau) \quad \# (1)$$

$$F_y = \omega^2 r \sin(\omega\tau) \quad \# (2)$$

where ω is the angular velocity of the microplate rotation (rad/s), r is the radius of rotation, which is 3mm, and t is the running duration (s).

2.3.3 Oxygen mass transfer model

$$a = \frac{A}{V} \quad \# (3)$$

where A is the gas-liquid interface area (m^2), V is the volume of liquid (m^3). There are many theories in the literature for the calculation of the transfer coefficient K_L , and this paper used the minimum eddy model proposed by Lamont and Scott [37]:

$$K_L = K \sqrt{D_L} \left(\frac{\epsilon}{\nu} \right) \quad \# (4)$$

where $K=0.4$ is the model constant. D_L is the diffusion coefficient of oxygen at $25^\circ C$, and ν is the kinematic viscosity of the liquid. When oxygen mass transfer in the microplate occurs at the gas-liquid interface, as oxygen mass transfer occurs at the interface, the local averaged energy dissipation ϵ shows better agreement with reported experimental data than volumetric averaged energy dissipation. So here, ϵ is the face average energy dissipation rate at the gas-liquid interface.

2.2.4 Mixing model

Volume power input and average energy dissipation are key parameters for microscale bioreactor mixing performance and fluid dynamics engineering [38]. The average energy dissipation rate ε can be represented by the following equation [39]:

$$\varepsilon = \frac{\mu\Phi\nu}{\rho} \# (5)$$

Volumetric power consumption is based on the energy expended by fluid motion and is expressed by the following equation [39]:

$$\frac{P}{V} = \frac{\int_{\vartheta} \mu\Phi\nu dV}{V} \# (6)$$

The μ in the above two equations is the kinematic viscosity of the fluid, and $\Phi\nu$ is the viscous dissipation function, which can be expressed in the study using the shear rate [39]:

$$\begin{aligned} \Phi\nu = 2 & \left[\left(\frac{\partial\mu}{\partial x} \right)^2 + \left(\frac{\partial v}{\partial y} \right)^2 + \left(\frac{\partial w}{\partial z} \right)^2 \right] \\ & + \left(\frac{\partial\mu}{\partial y} + \frac{\partial v}{\partial x} \right)^2 + \left(\frac{\partial v}{\partial z} + \frac{\partial w}{\partial y} \right)^2 + \left(\frac{\partial w}{\partial z} + \frac{\partial w}{\partial x} \right)^2 \# (7) \end{aligned}$$

The above equation can be transiently followed by parameters such as volumetric power input, interface area, oxygen mass transfer, etc., through which various indicators of microtiter plate vibration in the orbit can be monitored in real-time.

RESULTS AND DISCUSSION

3.1 Flow field prediction and CFD model validation

In order to test the reliability of CFD simulation and calculation algorithms, preliminary simulations were carried out, and the model was verified by comparing the K_{LA} and P/V results of the simulated gas-liquid interface with the results calculated by empirical formulas in the literature. The grid cells of the microtiter plates were divided into approximately 550,000 cells, with verified independence (**Fig.S1**). The results of the simulation were shown in **Figure 2**. It can be clearly seen in the **Figure 2A** and **2B** that the CFD simulation analysis results were very consistent with the results in the experimental literature. The predicted values differed from the results of the experiment, due to the slight differences in the fluid characteristics of the fermentation broth in experimental culture and the CFD. The liquid phase in the CFD simulation used the rheological properties of pure water, with a density (ρ) of 998.2 kg/m³, a viscosity (ϑ) of 0.01 m²/s, and a liquid surface tension (σ) of 0.0728 N/m. There was good consistency between the simulated value and the experimental value (p<0.05), indicating that the CFD model could realistically reflect the data in the experiment.

In addition, the flow field prediction diagram of microtiter plate sloshing was displayed by CFD to characterize the actual flow field at the gas-liquid interface. The specific movement of the liquid in the microplate was shown in **Figure 2**, with blue parts representing the liquid phase and red parts representing the gas phase. **Figure 2C** displayed the contours plot on the cross-section, and **Figure 2D** showed a three-dimensional motion model of the microtiter plate. By tracking its movement during orbital vibration, both figures clearly illustrated the real situation of fluid movement in the experiment. During the rotational movement, due to the action of centrifugal force, the liquid moved towards the wall, and the gas-liquid interface area increased rapidly under strong vibration conditions. After the orbital cycle was complete, the liquid

in the microplate circulated and reciprocated. Throughout the study, it was assumed that the gas-liquid interface was located on an iso-surface with a liquid phase volume fraction of 0.5. At the same time, the images of the movement track also verified the authenticity and reliability of the CFD model.

3.2 Performance evaluation of conventional microtiter plates

Most of the microtiter plates used in current studies have circular or square cross-sections. It has been proven that the oxygen transport efficiency of square cross-sectional microtiter plates is significantly higher than that of circular microtiter plates [40]. Therefore, only square cross-sectional microtiter plates were used in this section to explore and evaluate their performance during the culture and fermentation of strains. During experiments, the growth of microorganisms led to rheological changes in the fermentation broth. The changes in density, viscosity and surface tension must be considered during culture, in which the surface tension has a significant effect on the mass transfer efficiency between gas and liquid [41]. As shown in **Table 1**, the surface tension of the fermentation broth increased from 0.076 N/m to 0.103 N/m during the entire fermentation process. This rise had a significant impact on mass transfer and mixing performance between gas and liquid. Therefore, the phenomenon must be discussed in depth to explore the applicability of microtiter plates.

In this study, the changes in rheological properties of the fermentation broth of strains were simulated and analyzed in ANSYS Fluent. The simulated environment was performed at 300 rpm and 15% liquid load, and the results were shown in **Figure 3**. With the passage of culture time, the oxygen supply efficiency and mixing performance of the microtiter plate gradually decreased. The average turbulent dissipation rate (ϵ) also decreased from 0.45 m²/s³ at 0 h to 0.24 m²/s³ at 24 h, which greatly limited the growth of the microbes. The strain cultured in conventional microtiter plates was sampled after 24 hours, and it was observed microscopically that the biomass did not show a well-growing trend. The diameter of the cell was small, and the distribution was sparse. This growth condition resulted in low biomass and poor microbial activity, preventing the strains from meeting the needs of high-density fermentation, which would also have a negative impact on DHA production. Therefore, it is of great significance to optimize the existing microtiter plates to adapt to the culturing and screening of DHA producing strains.

3.3 New high-throughput bioreactor design

3.3.1 Reactor geometry design

Previous studies have demonstrated that the cross-sectional geometry of microtiter plates significantly affects their mass transfer and mixing properties [42]. In this section, the CFD technology was used to model microplates with different geometries and analyze them numerically, which explained the function and importance of geometry in microbial culture. **Figure 4A** presented a series of microtiter plate models with increasing edges, having a cross-sectional area limited to approximately 60 mm² and a total volume of 1.2 mL per titer. A vibration frequency of 150 rpm and a liquid charge of 15% were used for the numerical solution to ensure the consistency of reaction parameters. The influence of different reactor geometries was analyzed. Real-time monitoring of the microtiter plate's oxygen transport efficiency was performed using Equations 3 and 4 in Fluent, and its mixing performance was monitored in real-time using Equation 6. The results were output after 5 seconds of motion at a vibration radius of 3 mm, as shown in **Figure 4**.

The results of the calculation for mass transfer related parameters K_L , a , and $K_L a$ can be seen in **Figure 4B**. As the cross-sectional geometry of the microtiter plate changed from quadrilateral to hexagonal and gradually increased to circular, the data for oxygen transport efficiency fluctuated, with the relevant parameters reaching their highest values in the hexagonal microtiter plate. When the number of edges was increased from the conventional quadrangle to a regular hexagon, $K_L a$ rose significantly. Since K_L and a in the miniature vibrating bioreactor contributed almost equally to $K_L a$, the three parameters performed consistently. These parameters reflected the best performance in hexagonal microplates. In subsequent geometry modification, the mass transfer efficiency gradually decreased and finally reached a minimum oxygen transport efficiency

in the round microtiter plate, which was also consistent with other studies. The oxygen transfer efficiency of the square cross-sectional microtiter plate was significantly higher than that of the round microtiter plate, and the mass transfer related parameters of the round microplate were far inferior to those of other geometric reactors. In addition, the turbulent flow kinetic energy (k), turbulent energy dissipation rate and volumetric power consumption of the mixing performance were also characterized in **Figure 4C**. Similar to the changes in mass transfer parameters, as the number of sides of the reactor gradually increased from quadrilateral to hexagonal, the mixing performance was gradually optimized. Subsequently, in the regular heptagonal shape, the mixing performance continued to improve slightly, because more edges and corners affected the intensity of the internal movement. However, this would lead to the splash of fermentation broth in the experiment, increasing the risk of contamination. In simulations that continued to increase the number of microplate edges, this short-lived improvement in mixing performance disappeared and was replaced by a similar trend to the mass transfer parameters, which reached a minimum in round microplates. In conclusion, hexagonal microtiter plates showed superior mass transfer and mixing performance in the simulation, which laid the groundwork for future development of screening and culturing of DHA producing strains.

Moreover, the contour diagram of the gas-liquid interface of microplates in motion was characterized in CFD-Post to demonstrate the superiority of hexagonal microtiter plates in mass transfer and mixing performance (**Fig.S2**). The figure showed the differences in the speed of liquid movement in different geometries of microplates. In hexagonal microplates, the liquid had the fastest rate of movement. Additionally, the liquid movement trend in several microplates showed consistency. The movement speed near the bottom of the microtiter was low, while it was relatively high at the upper end. The specific movement of the liquid was caused by the applied centrifugal force. The superiority of the new bioreactor was also verified in the velocity contours of the liquid, which were consistent with the previous simulations. However, modifying the geometric shape of the microtiter plate alone is far from sufficient to meet the conditions of culturing and screening the DHA producing strains, and further improvements will be necessary in subsequent work.

3.3.2 Structure and reaction parameter optimization

In order to obtain optimal growth conditions, multiple parameters need to be optimized for the growth of DHA producing strains. However, gradually optimizing reaction parameters in software or experiments is a complex and difficult task. The mathematical and statistical response surface methodology (RSM) technique is a widely used method that consists of a set of mathematical techniques to describe the relationship between input and output parameters for modeling and optimization purposes. This RSM model estimates the combination of the input parameters yielding an optimal response through fast-running approximation of the simulation process [43]. In this study, the rotational speed, liquid filling volume and the number of baffles were regarded as three independent variables A, B and C, K_{La} and P/V were used as the result variables, and the RSM model was established based on the numerical calculation results of CFD. A complete experimental design matrix was given, and CFD-based simulation numerical experiments were carried out according to the experimental plan. The final results showed the effectiveness of each parameter and the influence of its interaction on the mass transfer and mixing performance. In subsequent work, ANOVA was performed to assess the quality of the developed model, as shown in **Table 2**. Based on a 95% confidence level, the results of the second-order quadratic models of K_{La} and P/V have significant F and P values (<0.05), which showed that the model constructed in this study was suitable for the range of variables studied. In the results of ANOVA in Table 2, the coefficients of determination R^2 were 0.9803 and 0.9775, indicating that the model had a perfect correlation between the independent variables and the response. The corrected R^2 were 0.9550 and 0.9486, indicating that only about 5% of the change could not be explained by the model.

The three-dimensional response surface was plotted based on the fitting second-order polynomial (**Fig.S3**). The influence of the baffle number, liquid charge and rotation speed on the changes of K_{La} and P/V was clear. Consequently, the interaction between the vibration velocity and the number of baffles significantly affects the mass transfer and mixing performance of the new bioreactor. The number of baffles and shaking frequency of the bioreactor were positively correlated with mass transfer and mixing. With the increase of the baffles and rotation speed, the performance of the bioreactor was gradually optimized. On the contrary,

the liquid filling volume was negatively correlated with the mass transfer and mixing performance, and the performance of the bioreactor tended to decrease with the increase of liquid load. The optimal conditions recommended by the CFD-based RSM model included 6 baffles, 15% liquid load, 800 rpm, maximum K_{La} level of 0.61 s^{-1} , and P/V of 2364 W/m^3 , which were sufficient to meet the growth conditions of DHA producing strains. The splashing phenomenon that might occur during the culture was also explained in subsequent model verification experiments. In summary, this study completed a method combined with the experimental design of the response surface on the framework of CFD technology to obtain the optimal culture conditions for DHA producing strains in a novel high-throughput bioreactor.

In this section, the superiority of the new high-throughput bioreactor for culturing and screening of DHA producing strains was established on the basis of CFD-RSM technology. Furthermore, simulation verification of CFD and experiments with solid microplates were conducted. The optimal reaction parameters given by the RSM model were numerically solved and compared for conventional quadrilateral microplates, hexagonal microplates, and the novel bioreactor using Fluent. The mass transfer and mixing levels of the new bioreactors were significantly higher than those of the other two microtiter plates. To further observe the superior performance of the new bioreactor, the liquid phase motion speed of the three microplates was derived in CFD-post. And planes of different heights were selected to reveal the distribution state of the liquid phase (**Fig.5**). **Figure 5A** showed that the motion state of liquid in the new bioreactor is more intense and uniform than that of the other two reactors, and the movement speed at parallel time is also significantly higher than that of the other two, which is conducive to the oxygen transport and nutrient absorption during the strain growth. In **Figure 5B**, several planes were selected inside the bioreactor. During the vibration movement, it was found that the liquid level height was higher in the new reactor. The closer it was to the ostiole, the better liquid phase distribution, compared with the other two reactors. The liquid phase distribution was more uniform in the new reactor rather than being limited to the wall surface, which attributed to the different geometric structure. All in all, the new bioreactor showed higher mixing and mass transfer levels than conventional reactors during simulations, and this improvement was sufficient to meet the culturing and screening needs of DHA producing strains.

3.4 Utilization of the novel microplate for screening DHA producing strains

Based on 3D modeling and printing technology, this study established and printed a new microtiter plate in equal scale. Three DHA producing strains stored in the laboratory were screened using the new microplate. The culture medium described above was used to cultivate the three strains in both conventional and novel microplates for 48 hours. The biomass of the fermentation broth was measured at 0, 12, 24, 36, and 48 hours. The results were shown in **Figure 6A**. The three species showed different growth states and trends over the culture time in the microplates. Under the same culture conditions, the three DHA-producing strains showed no significant difference in conventional microplates, and their biomass was lower than that of the novel microplates at the end of the culture. However, in the new microplates, the growth state and rate of *Schizochytrium* sp were significantly higher than those of the other two strains, and the biomass of *Schizochytrium* sp was 20% higher than that of *Aurantiochytrium* sp. and *Thraustochytrium* sp. at the end of culture. This phenomenon indicated that the oxygen level and mixing capacity provided by the new microtiter plate were better than those provided by the conventional microtiter plate in the process of constant temperature oscillation culture. There was no liquid spatter phenomenon during the entire culture process, which facilitated the growth of microorganisms. In addition, the new bioreactor had a larger cell diameter and higher cell density, while the conventional reactor had a small cell morphology and sparse cell density, due to oxygen dissolved limitation and uneven mixing during the culture process. In conclusion, the performance of the new bioreactor is significantly superior to that of the conventional bioreactor in both simulation experiments and laboratory experiments. In the process of vibration culture, it provides sufficient oxygen level and high mixing efficiency for the growth of strains, which is conducive to the high-throughput culturing and screening of high-yield DHA strains.

3.5 Optimization of culture conditions by novel microplates

On the basis of screening out a high-quality strain, the new microplate was used to optimize the culture medium in order to increase the DHA yield of fermentation. Design-Expert software was used to optimize the content of monosodium glutamate (MSG), yeast extract (Yeast) and glucose (Glu). Nile red staining reagent was used to quantitatively characterize the biomass, and the fluorescence intensity value was measured and used as the regulatory variable. The RSM model provided 17 kinds of experimental designs. Three groups of parallel experiments were conducted according to the recommended experimental design. After 48 h of culture, the samples of three groups were stained for measurement of fluorescence intensity (**Table 3**). Consequently, the optimal medium conditions included 20g/L MSG, 20g/L Yeast and 60g/L Glu. In order to verify the accuracy of the experimental design recommendation, at the end of the fermentation, the growth state of the strain was observed and recorded under a fluorescence microscope, as shown in **Figure 6B**. In the following work, Image J was used to process the pictures and calculate the average fluorescence density and the average diameter of the microorganisms under each different regulation medium state. The average fluorescence density represented the biomass of the strains, and the average diameter quantified the growth state of the strains. Considering the comprehensive comparison between the two parameters, the actual growth state of the strain under the regulation of the medium was observed, and the numerical results were shown in **Table 3**. The fluorescence images of the strains were consistent with the predictions of the RSM model. Under the recommended experimental design, the density and diameter of the strains were generally larger than those of other experimental designs. This study efficiently optimized the growth parameters of DHA-producing strain culture by using a newly designed microplate combined with response surface design, which is of great significance for guiding industrial fermentation for DHA in the future.

CONCLUSION

Based on CFD technology, a model was established to evaluate two important parameters, oxygen supply level and mixing efficiency of microtiter plates. The reliability of the model was verified by comparing it with the experimental literature data. In order to achieve high-throughput culturing and screening of DHA producing strains, the existing microplates were evaluated and modified. The superiority of microplates with hexagonal cross sections was determined. In the follow-up research, a high-precision RSM model based on the numerical calculation results of CFD was established. Baffles were introduced and reaction parameters (liquid filling volume and rotation speed) were optimized to improve oxygen transport and mixing efficiency in the new bioreactor. Finally, a hexagonal bioreactor with 6 baffles was developed. It has a liquid filling capacity of 15% and a rotation speed of 800 rpm. A K_{La} of 0.61 s^{-1} can be achieved, which is sufficient to meet the oxygen supply requirements of DHA producing strains, and provides the perfect mixing effect. This result was also verified in subsequent experiments and the liquid splashing problem was solved. The robustness of the strains was better than that under ordinary culture conditions. Furthermore, using the new microplate, a high-quality DHA producing strain was screened and the culture conditions were optimized. The new microtiter plate model designed in this paper provides not only a good model for the culture screening of DHA-producing strains but also a good new idea for the high-throughput culture screening of many high oxygen-consuming microorganisms in the future.

Acknowledgments

This work was financially supported by the National Natural Science Foundation of China (No. 22038007), the Jiangsu Provincial Natural Science Foundation (No. BK20200732).

Conflict of Interest Statement

The authors declare that they have no conflict of interests.

Data Availability Statement

The authors declared that the research data referred to correctly cited in the manuscript's reference section.

References

- [1] Du, Y. H., Wang, M. Y., Yang, L. H., Tong, L. L., *et al.* , Optimization and Scale-Up of Fermentation Processes Driven by Models. *Bioengineering (Basel)* 2022, *9* .
- [2] Liu, H., Qi, Y., Zhou, P., Ye, C., *et al.* , Microbial physiological engineering increases the efficiency of microbial cell factories. *Crit Rev Biotechnol* 2021, *41* , 339-354.
- [3] Orsi, E., Beekwilder, J., Eggink, G., Kengen, S. W. M., Weusthuis, R. A., The transition of *Rhodobacter sphaeroides* into a microbial cell factory. *Biotechnol Bioeng* 2021, *118* , 531-541.
- [4] Wang, Q., Han, W., Jin, W., Gao, S., Zhou, X., Docosahexaenoic acid production by *Schizochytrium* sp.: review and prospect. *Food Biotechnology* 2021, *35* , 111-135.
- [5] Zhang, Y., Wu, J., Mao, Z., Du, G., & Chen, J. (2017). High-throughput optimization of culture conditions for microbial fermentations using a microscale shake-flask array. *Biotechnology and bioengineering*, *114*(7), 1586-1594.
- [6] Zhang, X., Xie, N., Wang, Q., He, M., & Fang, J. (2021). High-throughput optimization of culture conditions and media composition for enhanced biosynthesis of coenzyme Q10 by *Rhodobacter sphaeroides*. *Bioprocess and Biosystems Engineering*, *44*(10), 2067-2081.
- [7] Wang, J., & Chen, Q. (2017). High-throughput screening and selection methods for cell line development. *Methods in molecular biology*, *1603*, 63-76.
- [8] Zhu, C., Wu, J., Li, H., & Li, X. (2021). A high-throughput, label-free, and real-time cell analysis platform based on impedance measurement for cell-based assay. *Analytical and bioanalytical chemistry*, *413*(16) , 4123-4133
- [9] Vormann, M. K., Gao, Y., Grass, M., & Eibl, D. (2019). High-throughput screening systems for micro-bioreactor cultivations. *Methods in molecular biology*, *1850*, 51-66.
- [10] Mears, L., Stocks, S. M., Albano, M., & Dikicioglu, D. (2020). Development of a novel microscale bioreactor system with integrated online monitoring for accelerated bioprocess development. *Biotechnology and bioengineering*, *117*(4), 1174-1184.
- [11] Huang, H., Zhang, L., & Mao, S. (2020). Recent advances and challenges in high-throughput screening platforms for microbioreactor-based fermentation process development. *Biotechnology advances*, *43*, 107596
- [12] Janzen, N. H., Franken, L. E., van Hest, J. C., & Cornelissen, J. J. (2020). Biodegradable polymeric nanoparticles based on diverse polyesters for theranostic applications. *Accounts of chemical research*, *53*(2) , 311-322.
- [13] Wutz, Robin Steiner, Kerstin Assfalg. (2018). Establishment of a CFD-based $k_L a$ model in microtiter plates to support CHO cell culture scale-up during clone selection. *AIChE Journal*, *5*, 1120-1128.
- [14] Zhang, X., He, Y., & Zhuang, Y. (2019). Advances in computational fluid dynamics simulations for bioprocess analysis and optimization. *Journal of industrial microbiology & biotechnology*, *46*(3-4), 399-412.
- [15] Huang, K., & Chen, Z. (2019). Computational fluid dynamics simulation for fermentation process in bioreactor: A review. *Biochemical Engineering Journal*, *147*, 10-23.
- [16] Amanullah, A., & Nienow, A. W. (2017). Computational fluid dynamics for the characterization, design, and optimization of bioreactors. *Biotechnology and Bioengineering*, *114*(10), 1905-1917.
- [17] Luo, X., & Chen, Z. (2018). Review of computational fluid dynamics in bioreactor hydrodynamics emphasizing mixing, particle suspension, and heat transfer. *Journal of chemical technology and biotechnology*, *93*(12), 3411-3422.

- [18] Kumar, D., & Chakraborty, S. (2019). Computational fluid dynamics (CFD) simulations in bioreactors: a review. *Journal of Chemical Technology and Biotechnology*, *94*(2), 403-422.
- [19] Hussain, A. A., Rahman, A. Y. A., & Aziz, A. R. A. (2020). A Review on Computational Fluid Dynamics and Its Application in Bioreactor Hydrodynamics. *In Computer-Aided Chemical Engineering*, *47*,1501-1506).
- [20] Singh, R. P., & Sharma, R. (2019). A review of recent advances in computational fluid dynamics for bioreactor design and optimization. *Journal of Chemical Technology and Biotechnology*, *94*(11),3455-3470.
- [21] Han, Y., & Song, J. (2020). The application of computational fluid dynamics in bioreactors: a review. *Journal of Bioscience and Bioengineering*, *129*(6), 653-667.
- [22] Li, X., Li, M., Tang, M., Li, X., & Zhang, Y. (2018). A high-throughput screening system for lipase engineering using the microfluidic droplet platform with an optical tweezers-based single droplet trapping. *Chemical Engineering Journal*, *343*, 654-661.
- [23] Phan, T. M., Duong, H. A., Lee, G. M., & Kim, D. H. (2019). Enhanced oxygen supply to high-density cultures of CHO cells in a 96-well microtiter plate using perfluorochemicals. *Biotechnology and bioengineering*, *116*(7), 1739-1747.
- [24] Wang, Y., Wu, X., Huang, P., Chen, J., Xiong, X., & Qian, L. (2021). Design and optimization of a new hybrid bioreactor with high-efficiency oxygen transfer and shear stress regulation. *Bioprocess and biosystems engineering*, *44*(10), 1569-1580.
- [25] Zhang, C., Wang, Y., Du, J., Guo, W., Liu, L., & Cao, X. (2016). Improving the oxygen transfer performance of 24-well microtiter plates by introducing baffles. *Journal of bioscience and bioengineering*, *122*(1), 83-88.
- [26] Kim, H. S., Yoo, M. J., Cho, J. H., & Lee, S. Y. (2015). Enhanced oxygen transfer in 96-deep well microtiter plates by applying agarose gel sealing method. *Biotechnology and bioprocess engineering*, *20*(1), 160-166.
- [27] Li, T., Li, Y., Li, J., Gao, C., & Ma, T. (2021). Microbial screening of renewable organic carbon sources in 96-well plates: experimental design, optimization and validation. *Frontiers in bioengineering and biotechnology*, *9*, 858.
- [28] Delgado G, Topete M, Galindo E. (1989). Interaction of cultural conditions and end-product distribution in *Bacillus subtilis* grown in shake flasks. *Appl Microbiol Biotechnol*, *31*, 288-292.
- [29] Jochen Büchs, Stefan Lotter, Claudia Milbradt. (2001). Out-of-phase operating conditions, a hitherto unknown phenomenon in shaking bioreactors. *Biochemical Engineering Journal*. *7*, 135-141.
- [30] Matthias Funke, Sylvia Diederichs, Frank Kensy, Carsten Muller, Jochen Büchs. (2009). The Baffled Microtiter Plate: Increased oxygen transfer and improved online monitoring in small scale fermentations. *Biotechnology and bioengineering*, *6*, 1118-1128.
- [31] Li, Q., Wang, L., & Cui, Z. (2017). Rheological measurements for bioprocessing: A review. *Biotechnology Journal*, *12*(6), 1600512.
- [32] Chen, J., Duan, Y., & Sun, Y. (2018). Rheological properties of microbial fermentation broths: A review. *Biotechnology Advances*, *36*(5) , 1515-1528.
- [33] Kothari, K., Natarajan, E., & Kumar, R. (2018). Simulation of gas-liquid interface dynamics in a bubble column using CFD. *Chemical Engineering Science*, *185*, 20-34.
- [34] Zhao, X., Shi, S., Wang, J., Xu, B., & Hu, Y. (2019). Numerical study on bubble dynamics in gas-liquid-solid three-phase flow using a Volume of Fluid (VOF) model. *Chemical Engineering Science*, *206*, 285-296.

[35] Yu Liu, Ze-Jian Wang, JianWen Zhang, Jian ye Xia, Ju Chu, Si-Liang Zhang, Ying Ping Zhuan. (2016). Quantitative evaluation of the shear threshold on *Carthamus tinctorius* L. cell growth with computational fluid dynamics in shaken flask bioreactors. *Biochemical Engineering Journal*, 113, 66-76.

[36] Agarwal, H., Kumar, R., & Singh, R. P. (2017). Optimization of oxygen transfer coefficient (K_{La}) for submerged fermentation of cellulase enzyme using response surface methodology. *Journal of microbiology and biotechnology research*, 7(2) , 20-27.

[37] Nobutaka Hanagata, Isao Karube. (1994). Red pigment production by *Carthamus tinctorius* cells in a two-stage culture system. *Journal of Biotechnology*, 1, 59-65.

[38] Astrid Dürauer, Stefanie Hobiger, Cornelia Walther, Alois Jungbauer. (2016). Mixing at the microscale: Power input in shaken microtiter plates. *Biotechnology Journal*, 11, 1539-1549.

[39] Hu Zhang, Sally R. Lamping, Samuel C.R. Pickering , Gary J. Lye, Parviz Ayazi Shamlou. Engineering characterisation of a single well from 24-well and 96-well microtitre plates. *Biochemical Engineering Journal*, 40, 138-149.

[40]Kamarajugadda, S., & Wells, A. (2013). Innovations in microplate technology for cell-based assays. *Assay and drug development technologies*, 11(5), 271-280.

[41] Tadayon, F., Mobasher, M. A., Naderi-Manesh, H., & Khajeh, K. (2019). Fermentation rheology and scaling up: A review. *Journal of Chemical Technology and Biotechnology*, 94(4) , 1007-1019.

[42] Jang, S. S., Kim, H. Y., Shin, J. H., Lee, S. H., & Lee, J. Y. (2019). Enhanced mass transfer performance of square-shaped microtiter plates for microbial cell culture. *Biochemical Engineering Journal*, 144 , 90-97.

[43] Pan, Y. J., Gagnon, P., & Huang, H. (2009). Statistical optimization of fed-batch culture of mammalian cells using response surface methodology. *Biotechnology progress*, 25(2) , 496-504.

Tables

Table1 Density \ viscosity and surface tension of strains fermentation broth at different time

Time/h	$\rho/\times\gamma\cdot\mu^{-3}$	$\mu/\Pi\alpha\cdot\varsigma$	$\sigma/N\cdot\mu^{-1}$
0	1078	0.003	0.076
8	1120	0.007	0.080
16	1194	0.024	0.092
24	1236	0.036	0.103

Table2 ANOVA results for the quadratic model - K_{La} and P/V responses.

	K_{La} response	K_{La} response	P/V response	P/V response
Source	P-Value	Significant	P-Value	Significant
Model	¡0.0001	Yes	¡0.0001	Yes
A	¡0.0001	Yes	¡0.0001	Yes
B	¡0.0001	Yes	¡0.0001	Yes
C	¡0.0001	Yes	¡0.0001	Yes
AB	0.1963	No	0.2450	No
AC	0.0035	Yes	0.0340	Yes
BC	0.0700	No	0.3871	No
A ²	0.2130	No	0.0039	Yes
B ²	0.0059	Yes	0.1098	No
C ²	0.1041	No	0.3998	No

K_{La} response	K_{La} response	P/V response	P/V response
$R^2=0.9803$	$R^2_{adj}=0.9550$	$R^2=0.9775$	$R^2_{adj}=0.9486$

Table 3. Results of medium optimization based on response surface

	MSG(g/L)	Yeast(g/L)	Glu(g/L)	Fluorescence intensity	Average fluorescence density	Average c
1	5	5	50	55685	144.27	7.67
2	20	5	50	64325	143.81	8.91
3	5	20	50	63521	166.92	7.68
4	20	20	60	68562	167.43	8.92
5	5	12.5	30	51246	143.51	7.35
6	20	12.5	30	56724	141.56	7.21
7	5	12.5	70	62897	154.36	8.51
8	20	12.5	70	65548	175.89	7.68
9	12.5	5	30	58798	167.81	8.25
10	12.5	20	30	59214	156.72	8.01
11	12.5	5	70	62528	176.87	7.98
12	12.5	20	70	64859	178.87	7.31
13	12.5	12.5	50	58210	158.34	8.83
14	12.5	12.5	50	64985	172.76	8.12
15	12.5	12.5	50	62098	176.46	7.67
16	12.5	12.5	50	60001	158.89	8.01
17	12.5	12.5	50	65254	167.88	8.25

Figure Legends

Figure 1 Schematic diagram of the new 96-well bioreactor.

Figure 2 CFD model validation and Flow field prediction. (A) Comparison of K_{La} from the literature and CFD results as a function of the shaking frequency. (B) Comparison of P/V from the literature and CFD results as a function of the shaking frequency. (C) Prediction of gas-liquid interface motion in the microtiter plate. (D) 3D model prediction of gas-liquid interface motion in the microtiter plate.

Figure 3 Changes of K_{La} and Turbulence Eddy Dissipation in microplates at different fermentation stages.

Figure 4 Design of the geometric structure of microplates. (A) A series of microplates with increasing edge numbers. (B) Mass transfer properties of microplates with different shapes. (C) Mixing parameters of microplates with different shapes.

Figure 5 Velocity contours and volume distribution of water in the original and novel microplates.

Figure 6 Screening and culture optimization of DHA-producing strains by novel microplates. (A) Changes in biomass of different strains: blue represents control group; red represents experimental group. (B) Results of fluorescent staining of the *Schizochytrium* sp.: the pictures represent the results for 4, 14, 2 and 9 in Table 3, respectively.

Figure 1

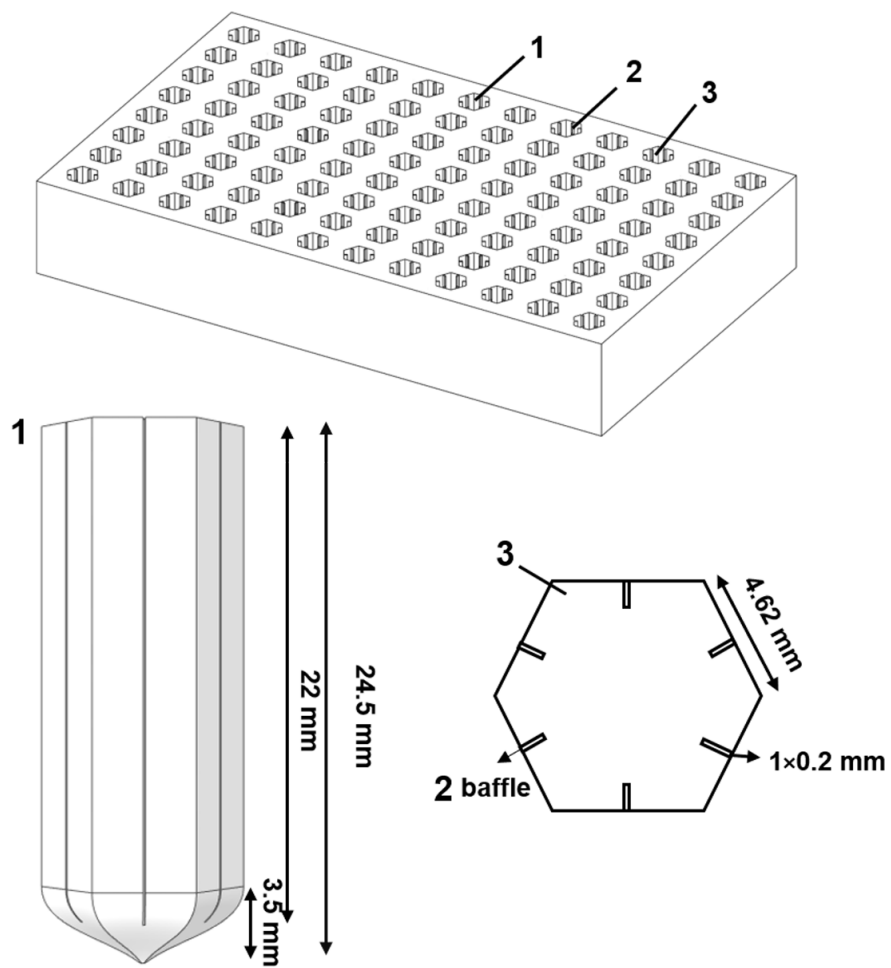


Figure 2

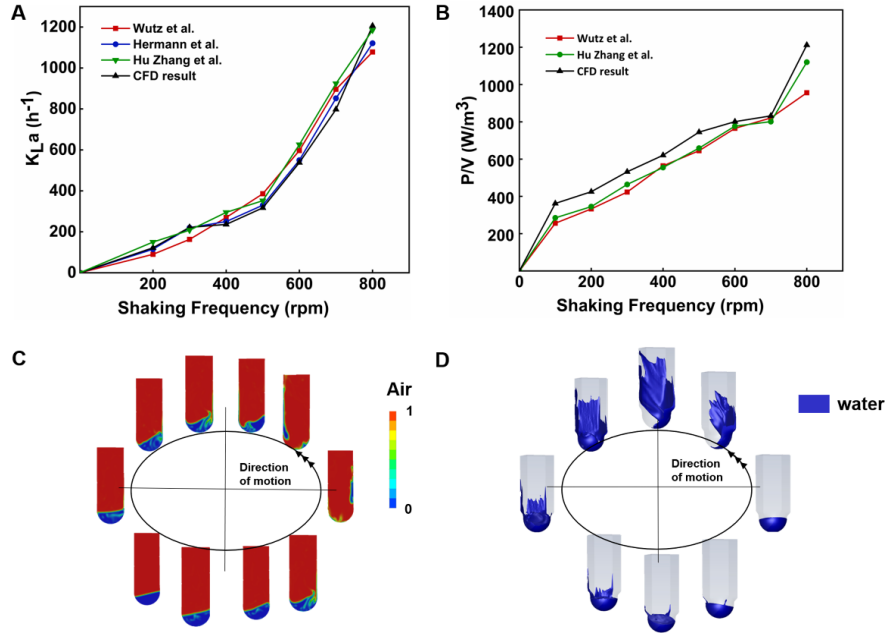


Figure 3

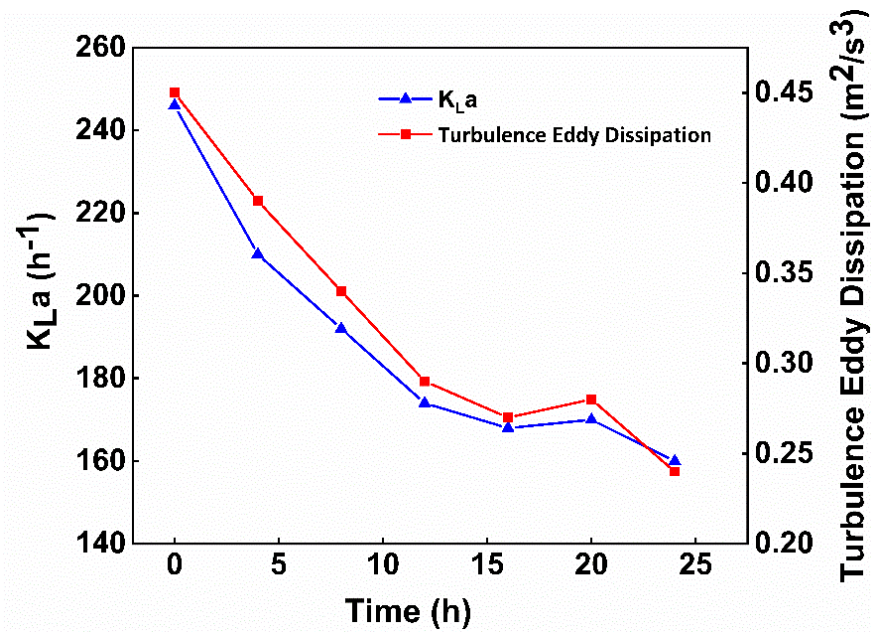


Figure 4

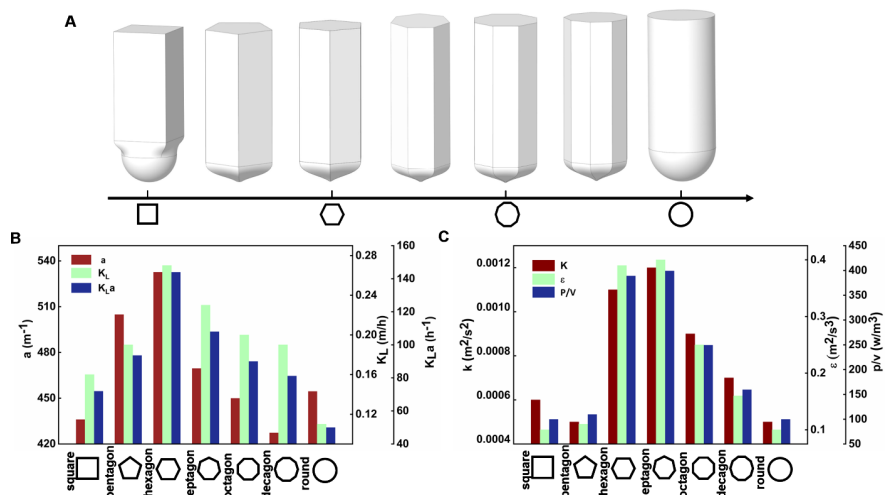


Figure 5

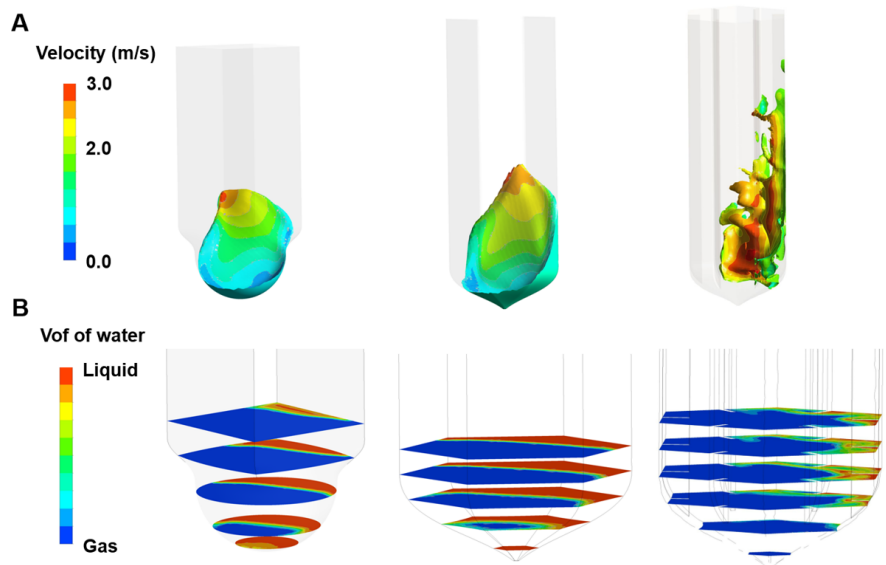


Figure 6

